

1                   **Modelling interactions of acid-base balance and respiratory status**  
2                   **in the toxicity of metal mixtures in the American oyster *Crassostrea virginica***

3  
4       Brett M. Macey<sup>a,b,h</sup>, Matthew J. Jenny<sup>g</sup>, Heidi R. Williams<sup>a,b</sup>, Lindy K. Thibodeaux<sup>a,b</sup>, Marion  
5       Beal<sup>a,c</sup>, Jonas S. Almeida<sup>d</sup>, Charles Cunningham<sup>a,d,f</sup>, Annalaura Mancia<sup>a,d</sup>, Gregory W. Warr<sup>a,d,i</sup>,  
6       Erin J. Burge<sup>a,b,e</sup>, A. Fred Holland<sup>a</sup>, Paul S. Gross<sup>a,d</sup>, Sonomi Hikima<sup>a,d</sup>, Karen G. Burnett<sup>a,b</sup>, and  
7                   Louis Burnett<sup>a,b</sup>, Robert W. Chapman<sup>a,b, c,d\*</sup>

8  
9       <sup>a</sup>Hollings Marine Laboratory (HML), Charleston, SC 29412, USA; <sup>b</sup>Grice Marine Laboratory,  
10       College of Charleston, Charleston, SC 29412, USA; <sup>c</sup>Marine Resources Research Institute, South  
11       Carolina Department of Natural Resources, Charleston, SC 29412, USA; <sup>d</sup>Medical University of  
12                   South Carolina, Charleston, SC 29425, USA

13       Current affiliations: <sup>e</sup>Department of Marine Science, Coastal Carolina University, Conway, SC  
14       29526, USA; <sup>f</sup>Department of Biology, University of New Mexico, Albuquerque, NM 87131,  
15       USA; <sup>g</sup>Woods Hole Oceanographic Institution, Woods Hole, MA 02543, USA; <sup>h</sup>Department of  
16       Environmental Affairs and Tourism, Marine and Coastal Management, Roggebaai 8012, RSA,  
17       <sup>i</sup>Division of Molecular and Cellular Biosciences, National Science Foundation, Arlington VA  
18                   22230.

19  
20  
21       \*Corresponding author: Hollings Marine Laboratory, 331 Fort Johnson Road, Charleston, South  
22       Carolina 29412; phone: (843)762-8860; fax: (843)762-8737; e-mail: [chapmanr@dnr.sc.gov](mailto:chapmanr@dnr.sc.gov)

23  
24       **Abbreviations:** ANN: artificial neural network; LPx: lipid peroxidation; TBARS: thiobarbituric  
25       acid-reactive substances; ROS: reactive oxygen species; THC: total hemocyte count; GSH:  
26       glutathione; TSA: tryptic soy agar; TCBS: thiosulfatecitrate-bile-sucrose; GLM: general linear  
27       models  
28

29

30 **Abstract**

31 Heavy metals, such as copper, zinc and cadmium, represent some of the most common and  
32 serious pollutants in coastal estuaries. In the present study, we used a combination of linear and  
33 artificial neural network (ANN) modelling to detect and explore interactions among low-dose  
34 mixtures of these heavy metals and their impacts on fundamental physiological processes in  
35 tissues of the Eastern oyster, *Crassostrea virginica*. Animals were exposed to Cd (0.001 – 0.400  
36  $\mu\text{M}$ ), Zn (0.001 – 3.059  $\mu\text{M}$ ) or Cu (0.002 – 0.787  $\mu\text{M}$ ), either alone or in combination for 1 to  
37 27 days. We measured indicators of acid-base balance (hemolymph pH and total  $\text{CO}_2$ ), gas  
38 exchange ( $\text{PO}_2$ ), immunocompetence (total hemocyte counts, numbers of invasive bacteria),  
39 antioxidant status (glutathione, GSH), oxidative damage (lipid peroxidation; LPx), and metal  
40 accumulation in the gill and the hepatopancreas. Linear analysis showed that oxidative  
41 membrane damage from tissue accumulation of environmental metals was correlated with  
42 impaired acid-base balance in oysters. ANN analysis revealed interactions of metals with  
43 hemolymph acid-base chemistry in predicting oxidative damage that were not evident from  
44 linear analyses. These results highlight the usefulness of machine learning approaches, such as  
45 ANNs, for improving our ability to recognize and understand the effects of sub-acute exposure to  
46 contaminant mixtures.

47

48 **Keywords:** heavy metals, artificial neural networks, *Crassostrea virginica*, lipid peroxidation,  
49 glutathione, acid-base balance, hemolymph  $\text{PO}_2$

50

51 **1. Introduction**

52

53 Industrialization and urbanization along the coastline of the US have substantially increased  
54 the amount and variety of anthropogenic pollutants entering estuarine ecosystems. Among the  
55 most common of these contaminants, heavy metals are of particular concern because they persist  
56 in the environment and have a wide variety of adverse effects. Developing biomarkers and  
57 predicting effects of contaminant mixtures, has garnered much attention in both human health

58 and ecological risk assessments (Carpenter et al. 2002; Yang et al. 2007; Wang et al. 2008) with  
59 the general recognition that the relationship among these mixture components and their  
60 biological effects is both intricate and complex (Sexton et al. 2007). For heavy metal mixtures  
61 this complexity is driven in part by the fact that many of these metals interact with a wide but  
62 common set of cellular targets, but may differ in affinity for these targets by many orders of  
63 magnitude (Viarengo 1989a).

64 We hypothesized that the relationship among heavy metals and their physiological effects  
65 might be detected and modelled using a combination of linear and artificial neural network  
66 (ANN) approaches. ANNs have been used to develop predictive models of other complex  
67 systems such climate change (Cannon et al. 2002, among others) and disease status in humans  
68 based upon gene expression profiles (Khan et al. 2001; Linder et al. 2004; Dankbar et al. 2007,  
69 among others).

70 To test this hypothesis, we characterized the physiological effects of environmentally-  
71 relevant low-dose mixtures of Cu, Cd, and Zn (Sanger et al. 1999), either alone or in  
72 combination for periods from 1 – 27 days, in the Eastern oyster, *Crassostrea virginica*. This  
73 ecologically and economically important bivalve mollusc lives in close association with  
74 estuarine sediments where its sessile nature and filter-feeding habit maximize the accumulation  
75 of contaminants in their tissues in concentrations high above those found in the surrounding  
76 seawater (Jenny et al. 2002).

77 In oysters, as in other organisms, Cu, Cd and Zn exist as divalent cations which are free or  
78 complexed to different classes of biological ligands. Cd is a trace metal with no known  
79 biological function, while Cu and Zn are essential elements and, as such, are required to maintain  
80 cellular homeostasis. In oysters, the gill and the hepatopancreas (digestive gland) are the  
81 primary tissues involved in the accumulation and detoxification of heavy metals, such as Cu, Zn  
82 and Cd (Marigómez et al. 2002; Sokolova et al. 2005). Heavy metals enhance the intracellular  
83 formation of toxic reactive oxygen species (ROS) (Stohs et al. 1995b; Ringwood et al. 1998;  
84 Geret et al. 2002b; Dailianis et al. 2005). Thus, metal-binding proteins and antioxidant enzymes,  
85 such as glutathione (GSH) and metallothioneins (MTs) are important detoxification elements that  
86 are induced to maintain the balance between pro- and antioxidative systems in cells (Dovzhenko  
87 et al. 2005). Indeed, studies have shown that surplus ROS can alter the structure of cell  
88 membranes by stimulating the peroxidation of membrane lipids. Thus, for the present study,

89 oysters were exposed to Cd, Zn, or Cu, either alone or in combination, for periods from 1 – 27  
90 days and indicators of antioxidant defense (GSH), oxidative damage (lipid peroxidation; LPx),  
91 immunocompetence (total hemocyte counts, numbers of invasive bacteria), as well as blood gas  
92 and acid-base balance (hemolymph PO<sub>2</sub>, pH, total CO<sub>2</sub>) were measured for each animal. The  
93 experimental design optimized input data for ANN analysis, which requires little or no  
94 understanding of the mechanistic associations of the measured variables, but does require  
95 considerable volumes of data. This design contrasts with traditional statistical approaches which  
96 require extensive knowledge of the system, but comparatively little data. Perhaps more  
97 succinctly traditional linear analysis fits data to models, but ANN's extracts models from data.  
98 ANN's do not require independence among the input variables (independent variables in linear  
99 regression). Furthermore, in the application of machine learning approaches, the preference is for  
100 limited or no replication of the experimental conditions, so the ANNs learn rather than  
101 memorize. For these and other reasons they have been used extensively in medical, engineering,  
102 physics and atmospheric sciences (Almeida, 2002, Cannon et al. 2002 Khan et al. 2001; Linder  
103 et al. 2004; Dankbar et al. 2007, Chapman *et al.* 2009) . Detailed explanations of the approach  
104 can be found in Bishop (1996a,b Bishop 2006). Our approach was a compromise between the  
105 requirements of linear statistics and of machine learning provided by ANNs. First, correlations  
106 among the experimental variables were examined by linear statistical tools to provide statistical  
107 power. Subsequently, ANN analysis was employed to explore the higher dimensional  
108 interactions among metal mixtures on the oyster's physiological response.

109

## 110 **2. Materials and Methods**

111

### 112 *2.1. Animal collection and maintenance*

113

114 Adult Eastern oysters, *Crassostrea virginica* (Gmelin), from Taylor Shellfish Farms  
115 (Shelton, WA) were held for 30 days in well-aerated recirculating natural seawater systems at 25  
116 ppt salinity and 20 – 22 ° C on a 12 h light cycle. During this period oysters were fed a mixed  
117 algal suspension (Shellfish Diet 1800<sup>®</sup>, Reed Mariculture) every second day.

118

### 119 *2.2. Basic experimental protocol*

120

121 One day prior to the start of the experiment, 4 oysters were placed in each of 54 five L  
122 beakers. Beakers contained four L of well-aerated filtered (0.45  $\mu\text{m}$ ) seawater maintained at 25  
123 ppt salinity and  $18 \pm 1$  °C. At the start of the 27 day experiment (Day 0), beakers were dosed  
124 with single or multiple metals at environmentally relevant doses (Table 1): Cd (0.001 – 0.400  
125  $\mu\text{M}$ ), Zn (0.001 – 3.059  $\mu\text{M}$ ) or Cu (0.002 – 0.787  $\mu\text{M}$ ). Thereafter, the seawater in each beaker  
126 was routinely exchanged every second day, at which time metals were replenished in each  
127 beaker to their predetermined concentrations, and algal suspension added to facilitate metal  
128 uptake by the oysters. Food was withheld from oysters at least 24 h before they were sampled.

129 Sampling of oysters began on day 1 of the 27 day metal study, with 1 oyster sampled per day  
130 from each of 8 beakers. Sampling began with beaker number one and continued to beaker 54,  
131 then back to beaker one, continuing for 27 days until all 216 samples had been exhausted. The  
132 study design was not consistent with a typical dose-response model based on linear statistics;  
133 instead this design generated 216 individual treatments that ultimately could be analyzed by  
134 ANNs. A total of 8 animals were found dead or moribund at the time of sampling; these oysters  
135 were not associated with any particular dosing regimen and were excluded from the study.

136 Each sampled oyster was blotted dry with a paper towel and weight, length, and width were  
137 recorded. Hemolymph (2 separate samples) was sampled anaerobically from the adductor  
138 muscle of each oyster using a 1 mL glass syringe fitted with a 23-ga needle. The dead space in  
139 the needle and syringe was filled with nitrogen-saturated distilled water to reduce contamination  
140 of the sample by atmospheric oxygen; the syringe was placed on ice prior to sampling. To gain  
141 access to the adductor muscle, the shell of the oyster was quickly notched along the posterior  
142 margin using pliers, exposing the muscle. Immediately following hemolymph withdrawal,  
143 oysters were placed on ice for dissection and tissue processing. Specific procedures are  
144 described below.

145

### 146 2.3. *Quantification of total hemocyte count (THC) and culturable bacteria in hemolymph*

147

148 Approximately 0.5 mL of hemolymph was withdrawn from the adductor muscle of each  
149 oyster. An aliquot of this sample was fixed with neutral buffered formaldehyde and hemocytes  
150 counted with a hemocytometer (Macey et al. 2008). For total counts of culturable bacteria, a

151 second aliquot of the original hemolymph sample was overlaid in marine agar on TSA  
152 supplemented with 2.0% NaCl; for total culturable *Vibrio*, a second 100  $\mu$ L aliquot of  
153 hemolymph was overlaid in marine again and cultured on TCBS agar supplemented with 1.5%  
154 NaCl (Macey et al. 2008). Data were expressed as total bacteria and *Vibrio* spp.  $\text{mL}^{-1}$  of  
155 hemolymph according to growth on TSA and TCBS plates, respectively.

156

#### 157 2.4. *Hemolymph variables*

158

159 A second hemolymph sample was withdrawn from the adductor muscle of each oyster to  
160 assess hemolymph gas and acid-base chemistry. All instruments were thermostatted to  $18 \pm 0.1$   
161  $^{\circ}\text{C}$ . The partial pressure of oxygen ( $\text{PO}_2$ ) in the hemolymph was determined with a Radiometer  
162 PHM pH/blood gas monitor and  $\text{PO}_2$  electrode. Hemolymph pH was determined with a  
163 Radiometer (BMS2 Mk2 Blood Micro System) capillary pH electrode and PHM pH/blood gas  
164 monitor that had been calibrated at experimental temperatures with precision Radiometer buffers.  
165 Total carbon dioxide, i.e., all forms of  $\text{CO}_2$  including molecular  $\text{CO}_2$ ,  $\text{HCO}_3^-$ ,  $\text{CO}_3^{=}$ , and  
166 carbamino  $\text{CO}_2$ , in the hemolymph was determined with a Capni-Con 5 total  $\text{CO}_2$  analyzer  
167 (Cameron Instrument Company).

168

#### 169 2.5. *Oyster dissection and tissue processing.*

170

171 The right valve of each oyster was removed by breaking the hinge of the shell and  
172 removing the gills and the hepatopancreas to separate weigh boats. Tissues were minced and  
173 approximately 0.02 g (minimum) and 0.05 g (maximum) samples of the minced tissues were  
174 transferred to separate cryotubes, flash frozen in liquid nitrogen and stored at  $-80^{\circ}\text{C}$  until they  
175 were used for the GSH, LPx and metal content assays (see below).

176

#### 177 2.6. *Lipid peroxidation (LPx) and glutathione (GSH) assays.*

178

179 Lipid peroxidation (LPx) in the gill and hepatopancreas of *C. virginica* was measured  
180 using a colorimetric assay that quantifies lipid degradation products based on the formation of  
181 total thiobarbituric acid reactive substances (TBARS) with malondialdehyde (TBARS) as the

182 standard (Ringwood et al. 1999b). GSH concentrations of individual oyster tissues were  
183 determined using the glutathione reductase recycling assay described by Ringwood et al.  
184 (1999b).

185

## 186 2.7. *Analysis of metal content*

187

188 Tissues were digested in concentrated nitric acid at 160 °C at 210 psi and 225 watt for 6  
189 min. Cooled samples were spiked with yttrium standard (10 ppm final concentration) and  
190 analyzed for Cu, Cd and Zn content by Inductively Coupled Plasma-Atomic Emission  
191 Spectroscopy. The National Bureau of Standards (NBS) Mussel Reference Material #1974b and  
192 Pygmy Sperm Whale Reference Material # QC03-LH3 were analysed with the samples to verify  
193 the metal analysis; the percent recoveries over all batches were  $101.67 \pm 11.74$ ,  $101.87 \pm 11.14$ ,  
194 and  $99.00 \pm 10.99\%$  (mean  $\pm$  S.D.) for Cu, Zn and Cd, respectively, for the Whale Reference  
195 Material and  $106.78 \pm 5.52$ ,  $95.74 \pm 4.70$ , and  $106.97 \pm 9.21\%$ , respectively, for the Mussel  
196 Reference Material. .

197

## 198 2.8. *Statistical analysis.*

199 . To determine the effect of metal exposure on the tissue accumulation of each metal and to  
200 assess potential relationships between tissue metal content and physiological responses, data  
201 were analyzed initially by linear statistics using SigmaStat 3.1 and SYSTAT 11 software.  
202 Correlations between tissue content of each metal and physiological measures were investigated  
203 using Pearson's Product Moment Correlation procedure. All tests for normality (Kolmogorov-  
204 Smirnov test) or equal variances failed, therefore, correlation analyses were performed on rank  
205 transformed data. One-way ANOVA was used to test for differences in concentrations of each  
206 metal between the gills and the hepatopancreas of oysters exposed to metals and was also used to  
207 test for differences between basal concentrations of each metal in each tissue of oysters not  
208 exposed to metals. All tests for normality or equal variances failed, therefore, a Kruskal-Wallis  
209 ANOVA on Ranks test was used to test for significant differences. Interactions between metal  
210 content of each tissue and physiological responses were assessed by analysis of variance  
211 (ANOVA) using General Linear Models (GLM) in SYSTAT 11. Since all test for normality and  
212 equal variance failed, GLM on quantile-normalized data were used to test for significant

213 interactions. Each GLM consisted of 3 independent variables [tissue (gill or hepatopancreas) Cu,  
214 Zn and Cd] and one dependent variable [tissue (gill or hepatopancreas) TBARS]. Significance  
215 was assigned at  $p \leq 0.05$  for all analyses. Subsequently, ANNs were used to model potential  
216 interactions of tissue metal contents and hemolymph measures in predicting tissue oxidative  
217 damage (LPx) or antioxidant status (GSH). Each of the ANNs consisted of 6 input variables  
218 [hemolymph pH, total CO<sub>2</sub>, PO<sub>2</sub>, and tissue (gill or hepatopancreas) Cu, Zn and Cd] with one  
219 output variable. For each output variable (gill LPx, gill GSH, hepatopancreas LPx and  
220 hepatopancreas GSH), separate ANNs (n = 30) were developed using WebNeuralNet 1.0  
221 (Almeida 2002). All variables were scaled to their non-parametric cumulative distributions by  
222 replacing the raw values with their rank/n (n = total data points) to overcome scale differences.  
223 The transformed data were then divided into two sets by random allocation; one comprising 90%  
224 of the records to train the ANN, while the remaining data were used as a cross validation (CV)  
225 set. A new subset of data was randomly selected before training each ANN to avoid bias in the  
226 selection of the CV set. Each ANN was first trained using both the input and output data of the  
227 training set, which consisted of 187 data points from each of the input and output variables. To  
228 prevent over training the ANNs, an early stopping procedure (Almeida 2002) was employed.  
229 After each ANN was trained, the withheld data points from the CV set were analyzed to evaluate  
230 the predictive capabilities of the ANN. In essence, this was achieved by calculating the R-  
231 squared (R<sup>2</sup>) values for the outputs of each ANN and the observed values of the accompanying  
232 CV sets, and comparing the CV set predictions with those generated by the appropriate ANN.  
233 Next, the impact of each input variable (hemolymph pH, total CO<sub>2</sub>, PO<sub>2</sub>, tissue Cu, Cd, Zn) was  
234 examined by computing the sensitivities of the outputs to changes in the inputs (Heshem, 1992)  
235 for all ANNs in which the model and CV set R<sup>2</sup> value were greater than the median value for all  
236 30 ANNs. The interactions of the inputs on the outputs were examined using a derivative of the  
237 approach of Cannon and McKendry (2002), where the two variables with the highest sensitivities  
238 were allowed to vary in 5% increments over the scaled range and all other input variables were  
239 held to their mean (50%) values. These ‘artificial’ data were then fed to the ANN models with  
240 the largest R<sup>2</sup> values to predict the output value and the results plotted on three-dimensional  
241 surfaces.

242

### 243 **3. Results**



244

245 3.1. *Metal accumulation in the tissues of C. virginica.*

246

247 Overall, measured concentrations of Cu, Cd and Zn ( $\mu\text{g g}^{-1}$  wet weight tissue) were  
248 higher in the hepatopancreas than in the gills of oysters exposed to metals (one-way ANOVA;  $P$   
249  $< 0.001$ ,  $< 0.001$ ,  $= 0.003$  and for Cu, Cd and Zn, respectively). Furthermore, basal  
250 concentrations of Cu and Zn were noticeably higher and more variable in the gills and the  
251 hepatopancreas when compared to basal Cd concentrations ( $P < 0.001$ ). Tissue levels of the  
252 essential metals Cu and Zn were independent of the ambient water concentrations of the metals  
253 over the entire range of exposures (Fig. 1A, B). In contrast, cadmium, a non-essential metal, was  
254 the only metal that accumulated linearly with time in the gill ( $r = 0.828$ ;  $P < 0.001$ ) and the  
255 hepatopancreas ( $r = 0.793$ ;  $P < 0.001$ ) over the full range of Cd exposure concentrations (Fig.  
256 1C). Cu contents were directly related to those of Zn in the gill ( $n = 208$ ,  $r = 0.0713$ ,  $P < 0.001$ )  
257 and in the hepatopancreas ( $n = 208$ ,  $r = 0.649$ ,  $P < 0.001$ ). To a lesser degree, Cu content  
258 positively correlated with Cd content in the gill ( $r = 0.216$ ,  $P = 0.0018$ ), but not in the  
259 hepatopancreas. No other significant correlations were observed between measured metals in  
260 either tissue.

261

262 3.2. *Correlation of measured tissue metals with physiological traits of C. virginica.*

263

264 Since each of the 216 test animals represented a unique set of metal exposure parameters  
265 (combination of metals, dose levels and duration), the resulting values could not be represented  
266 by standard descriptive statistics. Physiological data obtained from the 216 test animals (Figure  
267 2) generally fell within ranges reported for *C. virginica* in control or low level metal exposures  
268 (Viarengo et al. 1990; Roméo et al. 1997; Ringwood et al. 1998; Ringwood et al. 1999a).  
269 Correlations between metal exposures and physiological measures were investigated using  
270 Pearson's Product Moment Correlation procedure. Exposure to Zn was negatively correlated  
271 with TBARS, indicators of oxidative membrane damage in the hepatopancreas, ( $r = -0.150$ ,  $P =$   
272  $0.0304$ ), but not in the gill. No other significant relationships were noted between metal  
273 exposures and physiological measurements in oysters (data not shown). In contrast, tissue  
274 concentrations of individual metals were associated with several physiological measurements

275 (Fig. 3A, B), most notably TBARS. In the gill, Cu ( $r = 0.527$ ,  $P < 0.001$ ), Cd ( $r = 0.204$ ,  $P =$   
276  $0.0032$ ) and Zn ( $r = 0.256$ ,  $P < 0.001$ ) correlated positively with TBARS, as did Cu ( $r = 0.618$ ,  $P$   
277  $< 0.001$ ) and Zn ( $r = 0.247$ ,  $P < 0.001$ ) in the hepatopancreas. By comparison, metal associations  
278 with GSH were mixed. In the gill only Cu ( $r = 0.203$ ,  $P = 0.0033$ ) but not Zn or Cd positively  
279 correlated with antioxidant GSH, while both Cd ( $r = -0.149$ ,  $P < 0.001$ ) and Zn ( $r = -0.95$ ,  $P =$   
280  $0.0049$ ) in the hepatopancreas were negatively associated with GSH in that tissue.

281 Several other significant correlations were noted (Fig. 3A, B). Gill Cd was associated  
282 with increased hemolymph pH ( $r = 0.159$ ,  $p = 0.0221$ ) while hepatopancreas Cu correlated with  
283 increased hemolymph pH (and  $r = 0.284$ ,  $P < 0.001$ , respectively) and decreased total CO<sub>2</sub> ( $r =$   
284  $-0.137$ ,  $P = 0.0477$ ). Of the three metals, only Cu was associated with markers of immune  
285 function. Gill Cu was positively correlated with total culturable bacteria in the hemolymph ( $r =$   
286  $0.138$ ,  $P = 0.0461$ ), while hepatopancreas Cu was negatively associated with THC ( $r = -0.180$ ,  $P$   
287  $= 0.0092$ ).

288 In the hepatopancreas there was a significant interaction between measured Cu and Zn  
289 when predicting oxidative damage, measured as TBARS (Table 2, GLM,  $P = 0.014$ ), but not in  
290 the gill tissue. No additional significant interactions between the content of metals measured in  
291 gill and hepatopancreas were evident when predicting other physiological measurements of  
292 oysters, such as GSH, THC, hemolymph pH or total CO<sub>2</sub>.

293

### 294 3.3. *Artificial neural network analysis (ANN).*

295

296 Because interactions among the metals were detected by linear analysis, ANNs were used  
297 to explore these interactions in predicting LPx (measured as TBARS) in contrast to predicting  
298 GSH in the hepatopancreas and gill. The three respiratory measurements hemolymph pH, total  
299 CO<sub>2</sub> and PO<sub>2</sub> were included as input variables because the two acid-base components (pH, total  
300 CO<sub>2</sub>) responded to tissue contents of all three metals. ANN models could more reasonably  
301 predict hepatopancreas than gill TBARS based on the metal content of the respective tissues.  
302 The mean R<sup>2</sup> value for hepatopancreas TBARS over all the ANN models was  $0.50 \pm 0.11$  (Mean  
303  $\pm$  SD,  $n = 30$ ), with some of the values approaching 0.7 (Table 3). By comparison, the mean R<sup>2</sup>  
304 value for gill TBARS over all models was  $0.35 \pm 0.11$  (Table 4). Similarly, the cross-validation  
305 R<sup>2</sup> values for models predicting TBARS were  $0.53 \pm 0.14$  (Table 3) and  $0.24 \pm 0.16$  (Table 4) for

306 the hepatopancreas and the gills, respectively, confirming the relative validity of the predictions  
307 made by each model. Furthermore, hepatopancreas TBARS appeared to be more consistently  
308 predictable than gill TBARS, as the variation in  $R^2$  and cross-validation  $R^2$  values with respect to  
309 the mean in each model were smaller for the hepatopancreas than for the gills (Tables 3, 4).

310 In contrast, GSH in both the gills and the hepatopancreas was poorly predicted by the  
311 input variables used for ANN modelling. The mean  $R^2$  values for predicting GSH were only  
312  $0.07 \pm 0.06$  (Table 3) and  $0.14 \pm 0.11$  (Table 4) for the gills and the hepatopancreas, respectively.  
313 Likewise, the mean cross-validation  $R^2$  values and their variances for models predicting GSH in  
314 both tissue types were very low (Tables 3, 4).

315 A sensitivity analysis was conducted for the top performing ANNs to determine the  
316 contribution of each of the 6 input variables [hemolymph pH, total  $CO_2$ ,  $PO_2$ , and tissue (gill or  
317 hepatopancreas) Cu, Cd or Zn] to the overall variance observed in each model predicting tissue  
318 TBARS. As GSH was poorly predicted by all ANN models in the present study, a sensitivity  
319 analysis was not conducted for these models. The best performing ANNs had model and cross-  
320 validation  $R^2$  values greater than the median value for all 30 ANNs. Models 6 and 7 were chosen  
321 from the ANNs predicting hepatopancreas TBARS (Table 3), while Model 8 was chosen from  
322 ANNs predicting gill TBARS (Table 4). Sensitivity analysis reveals that in the hepatopancreas,  
323 the partial pressure of oxygen ( $PO_2$ ) in the hemolymph is a dominant variable in both models  
324 (Fig. 4). Model 6 has the larger mean  $R^2$  value. Model 7 has the larger cross-validation  $R^2$  value  
325 and a smaller number of nodes (Table 4) and in most cases we would choose Model 7 over 6 for  
326 these reasons. However, as Model 6 indicates that Cu is more important than Zn in predicting  
327 TBARS (indicating LPx) and as this model confirms findings from the linear statistical analysis,  
328 we would suggest that this is the preferred ANN model. Model 6 suggests that LPx in the  
329 hepatopancreas is more sensitive to changes in tissue Cu and Cd, and to hemolymph  $PO_2$ , than to  
330 any of the other measured variables (Fig. 4).

331 Sensitivity analysis indicated that each of the input variables contributed to the overall  
332 variance observed in Model 8 in predicting gill TBARS (Fig. 5). In the gill, as in the  
333 hepatopancreas, it is clear that the degree of oxidative membrane damage is more sensitive to  
334 changes in tissue Cu than to other input variables, but hemolymph pH, total  $CO_2$  and  $PO_2$  also  
335 make strong contributions to predicting TBARS. Moreover, summed Cu, Zn and Cd  
336 concentrations in both tissues appear to make significant contributions towards the overall

337 variance observed in each model, emphasizing the cumulative detrimental effects of these metals  
338 on membrane integrity.

339 The interactions of the more sensitive input variables (tissue Cu, hemolymph pH and  
340 hemolymph PO<sub>2</sub>) in predicting TBARS in the gills and the hepatopancreas were graphically  
341 illustrated (Fig. 6A, B) using a modified form of the sensitivity analysis described by Cannon  
342 and McKendry (2002). Oxidative damage in the gill (TBARS) increased as hemolymph pH and  
343 tissue Cu concentrations increased and the effects are non-linear, but not strongly so (Fig. 6A).  
344 Similarly, hepatopancreas TBARS increased with increasing PO<sub>2</sub> in the hemolymph and with  
345 hepatopancreas Cu (Fig. 6B). These graphical surfaces clearly suggest complex, non-linear  
346 interactions between tissue Cu content and hemolymph pH or PO<sub>2</sub> in predicting tissue TBARS.  
347 Furthermore, the overall TBARS response is consistent with an increasingly oxidative  
348 environment.

349

#### 350 **4. Discussion**

351

352 ANN models generated in the present study demonstrated that the responses of key  
353 toxicological indicators can be modelled and predicted from an appropriate set of input variables.  
354 While linear analyses provided correlative values of some individual metals to changes in  
355 hemolymph gasses and pH, ANN analysis suggested that the level of damage to cellular  
356 membranes was sensitive to tissue content of all three metals and strongly depended on other  
357 physiological measures, such as changes in hemolymph pH and PO<sub>2</sub> (Fig. 6). To our knowledge,  
358 this is the first study to show important metal-metal interactions as well as interactions of metal  
359 content with hemolymph gas and acid-base chemistry in predicting membrane damage in  
360 molluscs. It is particularly noteworthy that where low tissue Cu is accompanied by low pH or  
361 low PO<sub>2</sub> both hepatopancreas and gill manifest the lowest predicted level of TBARS, while in  
362 those tissues with high Cu content along with high pH or high PO<sub>2</sub>, the reverse is observed (Fig.  
363 6). This is in keeping with our understanding of the response of TBARS to redox conditions,  
364 and the overall topography of the predicted response clearly suggests a non-linear interaction  
365 between metal content, hemolymph acid-base variables and TBARS. The contributions of  
366 hemolymph variables to the predictive power of the ANN models as observed in the present  
367 study could be explained by changes in ventilation rate of oysters as function of metal exposure

368 or tissue burden, as reported for tropical oysters *Crassostrea belcheri* exposed to Cu (Elfwing et  
369 al. 2002). Alternatively, tissue metal burdens may be limited by ventilatory activity in bivalves  
370 as reported for Cd uptake in the Asiatic clam, *Corbicula fluminea* (Massabuau et al. 2003).  
371 Certainly, the resulting changes in gas exchange and acid-base physiology of oysters could  
372 influence a variety of biochemical processes, including the deposition of shell that is essential to  
373 oyster growth (Booth et al. 1984; Burnett 1988).

374 While linear regression techniques can generate response-surface plots, they cannot  
375 interrogate non-linear dynamics similar to those in Fig 6 without human intervention specifying  
376 the structure of the relationships. The advantage of the ANN's is that the mathematical  
377 architecture is infinitely flexible and does not require human intervention (eg. bias). The various  
378 models produced by the analysis are not viewed as solutions, but rather as hypotheses of  
379 relationships amenable to further empirical tests.

380 In the present study, Cu, Zn and Cd tissue contents correlated with significant changes in  
381 LPx, as measured by elevated tissue levels of total TBARS. The influence of transition metals  
382 such as Cu on oxidative processes, resulting in the production of oxyradicals, has been described,  
383 and it is suggested that cupric ions are involved in both the initiation and propagation steps of  
384 LPx (reviewed by Viarengo 1989a). In fact, increases in LPx following exposure to Cu have  
385 been documented in the hard clam *Ruditapes decussatus* (Roméo et al. 1997), the Eastern oyster  
386 *Crassostrea virginica* (Ringwood et al. 1998), and the mussels *Mytilus galloprovincialis*  
387 (Viarengo et al. 1990) and *Mytilus edulis* (Geret et al. 2002a). While excess Cu can mediate free  
388 radical production directly via redox cycling, oxyradicals may also be formed indirectly via  
389 cupric ions binding to and adversely affecting metal-requiring antioxidants, such as GSH and  
390 MT (Ringwood et al. 1999a; Valko et al. 2005). In fact, it has been strongly suggested that there  
391 are multiple processes that bind copper and reduce its cellular toxicity (Valko et al. 2005).  
392 Conversely, non-redox metals, such as Cd, are unable to generate free radicals directly and  
393 indirectly cause free radical-induced damage to important cellular macromolecules, particularly  
394 various complexes of the electron transport chain in mitochondria, and inhibit important cellular  
395 antioxidant enzymes and proteins, which may, in turn, stimulate LPx through oxidation of  
396 polyunsaturated fatty acids (Stohs et al. 1995a; Stohs et al. 2000; Dorta et al. 2003; Wang et al.  
397 2004). The inverse association of Zn and Cd with GSH in the hepatopancreas observed in our  
398 study supports the idea that GSH provides early protection against oxidative stress from

399 exposure to these metals, by binding of these metals to GSH or inhibition of GSH synthesis by  
400 these metals, until MTs can be induced (Quig 1998; Ringwood et al. 1998). That this effect was  
401 not noted for Cu in this study supports the notion that Cu ions, which can undergo redox cycling,  
402 are involved in both the initiation and propagation steps of LPx via the direct formation of  
403 reactive oxygen species, whereas Cd and Zn ions, which do not undergo redox cycling, stimulate  
404 LPx indirectly by binding to and inhibiting cellular antioxidants, such as GSH (Viarengo 1989a).  
405 This does not however exclude the possibility of the formation of Cu-GSH complexes,  
406 particularly since –SH groups of most metabolites and enzymes, including GSH, have a higher  
407 affinity for Cu than Cd or Zn (Viarengo 1989b). In fact, the discovery that the upper limit of  
408 “free” pools of Cu are far less than a single ion per cell strongly suggests that there is significant  
409 overcapacity for chelation of Cu in the cell and that multiple cellular antioxidants exist that bind  
410 Cu (Valko et al. 2005). However, Ringwood et al. (Ringwood et al. 1998) suggested that  
411 conditions that cause depletion of important cellular antioxidants, such as GSH and MT, may  
412 enhance pollutant toxicity, suggesting that the impacts of exposure to metal mixtures are  
413 complex and potentially compounding. Indeed, the significant correlation between tissue  
414 contents of Cd and LPx as well as the general linear model identification of Zn-Cu interactions in  
415 predicting LPx of oysters in the present study supports this notion.

416 Cd suppresses the activity of many antioxidant enzymes and can displace Cu and Fe from  
417 cytoplasmic and membrane proteins which may then participate in ROS-producing Fenton  
418 reactions (Flipič et al. 2006). More specifically, Engel (1999) demonstrated that Cu can displace  
419 Cd from MT when oysters are exposed to these trace metals in combination, but that Cd is not  
420 lost from the tissues of the oyster. Furthermore, it is postulated that MT gene expression in  
421 oysters is regulated via a Zn-sensitive inhibitor, as is the case for regulation of MT gene  
422 expression in mice (Roesijadi 1996). Although MT induction via the displacement of Zn has yet  
423 to be empirically demonstrated in oysters, it is possible that this sort of metal-metal exchange  
424 reaction is responsible for the Zn-Cu interactions observed in oysters in the present study when  
425 predicting tissue LPx.

426 The approach of combining general linear models and ANN analysis has revealed  
427 important metal-metal interactions as well as interactions of metal content with hemolymph gas  
428 and acid-base chemistry (hemolymph PO<sub>2</sub> as well as pH and total CO<sub>2</sub>) in predicting peroxidation  
429 of membrane lipids that were not evident from linear analyses. These results support a growing

430 body of evidence implicating the role of heavy metals in the peroxidation of membrane lipids  
431 and the disruption of important cellular antioxidants that play key roles in protecting cells against  
432 oxidative damage. This study also highlights the usefulness of machine learning approaches,  
433 such as ANNs, for improving our ability to recognize and understand the effects of sub-acute  
434 exposure to environmentally relevant concentrations of mixed contaminants.

435

## 436 **5. Acknowledgements**

437

438 This study was supported by NOAA's Center of Excellence in Oceans and Human Health  
439 at HML and the National Science Foundation. Any opinion, finding, conclusions or  
440 recommendations expressed in this material are those of the authors and do not necessarily  
441 reflect the views of the NSF. GML Contribution No. 348; MRD SCDNR Contribution ####.

442

443 **Tables**

444 **Table 1.** Concentrations ( $\mu\text{M}$ ) of  $\text{CuCl}_2$ ,  $\text{ZnCl}_2$  and  $\text{CdCl}_2$  added to each beaker during the 27  
445 day oyster metal challenge experiment.

446	<b>Beaker #</b>	<b>Zinc</b>	<b>Copper</b>	<b>Cadmium</b>
447	1	0.049	0.000	0.214
448	2	0.196	0.315	0.000
449	3	0.306	0.002	0.037
450	4	1.101	0.066	0.044
451	5	3.059	0.044	0.010
452	6	0.000	0.000	0.000
453	7	2.447	0.050	0.000
454	8	0.000	0.197	0.013
455	9	0.092	0.000	0.062
456	10	0.000	0.000	0.025
457	11	0.306	0.079	0.000
458	12	1.835	0.598	0.267
459	13	1.590	0.787	0.002
460	14	0.000	0.039	0.004
461	15	1.223	0.017	0.231
462	16	2.080	0.000	0.004
463	17	0.000	0.010	0.006
464	18	0.000	0.000	0.000
465	19	0.765	0.000	0.111
466	20	0.000	0.220	0.400
467	21	0.040	0.000	0.044
468	22	0.000	0.000	0.000
469	23	0.000	0.000	0.302
470	24	0.979	0.409	0.000
471	25	0.031	0.008	0.004
472	26	0.171	0.504	0.178
473	27	0.428	0.000	0.000
474	28	0.000	0.252	0.445
475	29	0.015	0.004	0.125
476	30	0.012	0.000	0.000
477	31	0.000	0.000	0.160
478	32	0.110	0.028	0.016
479	33	1.468	0.110	0.001
480	34	2.325	0.007	0.000
481	35	0.006	0.472	0.320
482	36	2.753	0.000	0.000
483	37	0.000	0.003	0.000
484	38	0.000	0.013	0.338
485	39	0.000	0.001	0.000
486	40	2.202	0.000	0.028
487	41	0.000	0.157	0.007



488	42	0.000	0.024	0.356
489	43	0.003	0.000	0.000
490	44	0.028	0.283	0.000
491	45	0.067	0.567	0.007
492	46	0.000	0.708	0.000
493	47	0.153	0.006	0.000
494	48	0.612	0.000	0.089
495	49	0.000	0.079	0.000
496	50	1.957	0.629	0.285
497	51	0.049	0.013	0.142
498	52	0.257	0.535	0.002
499	53	0.856	0.378	0.000
500	54	0.024	0.000	0.022
501				

502 **Table 2.** Assessment of interactions between metal contents of hepatopancreas when predicting  
 503 oxidation damage, measured as TBARS (General Linear Models). \* significant interactions  
 504 (P<0.05).

505	506	Coefficient	STD Error	STD	Tolerance	t	P(2 Tail)
507				<b>Coefficient</b>			
508	Constant	2.894	10.174	0.000	.0284	0.777	
509	Cu	1.309	0.416	1.309	0.045	3.149	0.003*
510	Zn	0.777	0.399	0.777	0.049	1.949	0.056
511	Cd	-0.043	0.276	-0.043	0.102	-0.156	0.877
512	Cu*Zn	-0.026	0.010	-1.668	0.018	-2.525	0.014*
513	Cu*Cd	-0.004	0.011	-0.207	0.024	-0.360	0.720
514	Zn*Cd	-0.015	0.011	-0.809	0.022	-1.346	0.183
515	Cu*Zn*Cd	0.00	0.000	1.251	0.011	1.515	0.135
516							

517 **Table 3.** ANN (n = 30) analysis of TBARS and GSH levels in the hepatopancreas of oysters  
 518 exposed to Cu, Zn and/or Cd.

519	<b>Lipid Peroxidation (TBARS)</b>				<b>Glutathione (GSH)</b>		
520	<b>Model</b>	<b># Nodes</b>	<b>Model R2</b>	<b>CV R2</b>	<b>#Nodes</b>	<b>Model R2</b>	<b>CV R2</b>
521	1	9	0.4289	0.2652	9	0.1349	0.0866
522	2	9	0.3715	0.7326	7	0.1441	0.1110
523	3	5	0.6957	0.3642	5	0.3667	0.1649
524	4	7	0.5006	0.4938	5	0.0864	0.0328
525	5	7	0.3917	0.6919	5	0.0720	0.2296
526	6	7	0.6465	0.4681	7	0.1176	0.1654
527	7	5	0.6072	0.7002	7	0.3028	0.0688
528	8	5	0.3979	0.6905	9	0.1172	0.3552
529	9	7	0.5649	0.7380	6	0.3948	0.0058
530	10	5	0.6035	0.6459	7	0.0586	0.1656
531	11	6	0.6075	0.5286	5	0.1056	0.2849
532	12	5	0.6124	0.6212	11	0.1279	0.3194
533	13	7	0.4208	0.8799	7	0.1111	0.0151
534	14	5	0.3779	0.5179	5	0.0775	0.0807
535	15	5	0.4201	0.6586	7	0.1033	0.2656
536	16	5	0.4052	0.5568	5	0.3134	0.3727
537	17	5	0.6587	0.3128	5	0.2803	0.1421
538	18	5	0.6269	0.4792	5	0.0992	0.1796
539	19	5	0.2801	0.5103	8	0.1201	0.1013
540	20	6	0.4136	0.5071	5	0.0255	0.2573
541	21	5	0.6408	0.3670	9	0.1422	0.0052
542	22	5	0.3890	0.5743	5	0.3510	0.4110
543	23	5	0.6245	0.4559	6	0.1006	0.0303
544	24	5	0.5942	0.4939	7	0.0676	0.0754
545	25	5	0.4384	0.4662	5	0.1239	0.0052
546	26	5	0.4184	0.4533	6	0.3116	0.0455
547	27	7	0.5060	0.5056	5	0.0111	0.0003
548	28	5	0.4105	0.6626	5	0.0197	0.0169
549	29	5	0.3373	0.3752	6	0.1104	0.0000
550	30	7	0.6149	0.2975	5	0.0427	0.0432
551	<b>Mean</b>	<b>5.8000</b>	<b>0.5002</b>	<b>0.5338</b>	<b>6.3000</b>	<b>0.1480</b>	<b>0.1346</b>
552	<b>SD</b>	<b>1.2149</b>	<b>0.1178</b>	<b>0.1464</b>	<b>1.6006</b>	<b>0.1100</b>	<b>0.1247</b>

553 **Table 4.** ANN (n = 30) analysis of TBARS and GSH levels in the gills of oysters exposed to  
 554 Cu, Zn and/or Cd.

555	<b>Lipid Peroxidation (TBARS)</b>				<b>Glutathione (GSH)</b>		
556	<b>Model</b>	<b>#Nodes</b>	<b>Model R2</b>	<b>CV R2</b>	<b>#Nodes</b>	<b>Model R2</b>	<b>CV R2</b>
557	1	5	0.2538	0.0007	9	0.0797	0.0154
558	2	7	0.2423	0.1488	7	0.0179	0.0647
559	3	7	0.2578	0.4011	9	0.0635	0.0173
560	4	6	0.2405	0.1909	5	0.0029	0.0504
561	5	5	0.1802	0.3001	7	0.0314	0.0003
562	6	7	0.2687	0.4040	7	0.0726	0.0044
563	7	8	0.3386	0.2644	8	0.0843	0.0459
564	8	8	0.4818	0.2464	5	0.0471	0.0413
565	9	7	0.1684	0.0625	10	0.0697	0.0393
566	10	11	0.4871	0.2322	9	0.2961	0.0250
567	11	5	0.4528	0.2011	7	0.0223	0.1310
568	12	6	0.2826	0.4182	7	0.0674	0.0007
569	13	6	0.4153	0.4901	6	0.0178	0.1964
570	14	5	0.5444	0.0489	5	0.0526	0.0022
571	15	7	0.4401	0.1768	5	0.0498	0.1191
572	16	8	0.3297	0.2637	11	0.0588	0.0771
573	17	5	0.4234	0.4465	6	0.0650	0.1535
574	18	7	0.5074	0.1323	6	0.0344	0.0139
575	19	9	0.3102	0.1496	7	0.1644	0.0249
576	20	5	0.3989	0.4732	5	0.0346	0.0899
577	21	8	0.2456	0.3080	7	0.0346	0.0029
578	22	5	0.3934	0.5798	5	0.0758	0.0025
579	23	5	0.5077	0.0112	7	0.0554	0.0097
580	24	5	0.1863	0.2495	5	0.0793	0.0159
581	25	5	0.3005	0.0058	8	0.0431	0.0394
582	26	7	0.2522	0.1038	10	0.0694	0.0328
583	27	9	0.2899	0.3309	11	0.0732	0.0266
584	28	5	0.2295	0.2209	9	0.1984	0.0519
585	29	5	0.4402	0.5114	7	0.1516	0.0122
586	30	5	0.5173	0.0320	8	0.0652	0.1652
587	<b>Mean</b>	<b>6.4333</b>	<b>0.3462</b>	<b>0.2468</b>	<b>7.2667</b>	<b>0.0726</b>	<b>0.0491</b>
588	<b>SD</b>	<b>1.5906</b>	<b>0.1139</b>	<b>0.1641</b>	<b>1.8370</b>	<b>0.0597</b>	<b>0.0536</b>
589							

590 **Figure Legends**

591 **Figure 1.** (A) The tissue concentrations of Cu measured in the gill and the hepatopancreas of  
592 *Crassostrea virginica* held in Cu alone or in combination with other metals for 1 – 27 days.  
593 Total waterborne exposure to Cu (x-axis) is expressed as water concentration of Cu ( $\mu\text{M}$ ) \*days  
594 of exposure. Concentrations of Zn (B) and Cd (C) in the same tissues are displayed as a  
595 function of total waterborne exposure to Zn and Cd, respectively.

596

597 **Figure 2.** Box-and-whiskers plots of data from all experimental animals ( $n = 208$ ) for each  
598 major physiological variable measured in this study. (A) TBARS and GSH values for the gill  
599 and the hepatopancreas (Hepato), (B) total hemocyte count (THC), (C) hemolymph  $\text{PO}_2$  and total  
600  $\text{CO}_2$ , (D) hemolymph pH, and (E) colony-forming units (CFU)  $\text{mL}^{-1}$  hemolymph on TSA or  
601 TCBS agar. Box boundaries indicate 25<sup>th</sup> and 75<sup>th</sup> percentile, the line within the box marks the  
602 median value, and whiskers indicate the 10<sup>th</sup> and 90<sup>th</sup> percentiles. All values, including outliers  
603 are depicted.

604

605 **Figure 3.** Correlation coefficients (r-values) for significant associations between physiological  
606 measurements and measured metals in (A) the gill and (B) the hepatopancreas of *Crassostrea*  
607 *virginica* following exposure to each metal alone and in combinations for a period of 1 – 27  
608 days. Analysis was performed using the Pearson Product Moment Correlation procedure on rank  
609 transformed data and significance was assigned at  $P < 0.05$ . Non-significant interactions are not  
610 shown.

611

612 **Figure 4.** Sensitivities of TBARS in hepatopancreas to the input variables (metal contents,  
613 hemolymph pH, PO<sub>2</sub> and total CO<sub>2</sub>) for the best performing models 6 and 7 from the ANN  
614 analysis.

615

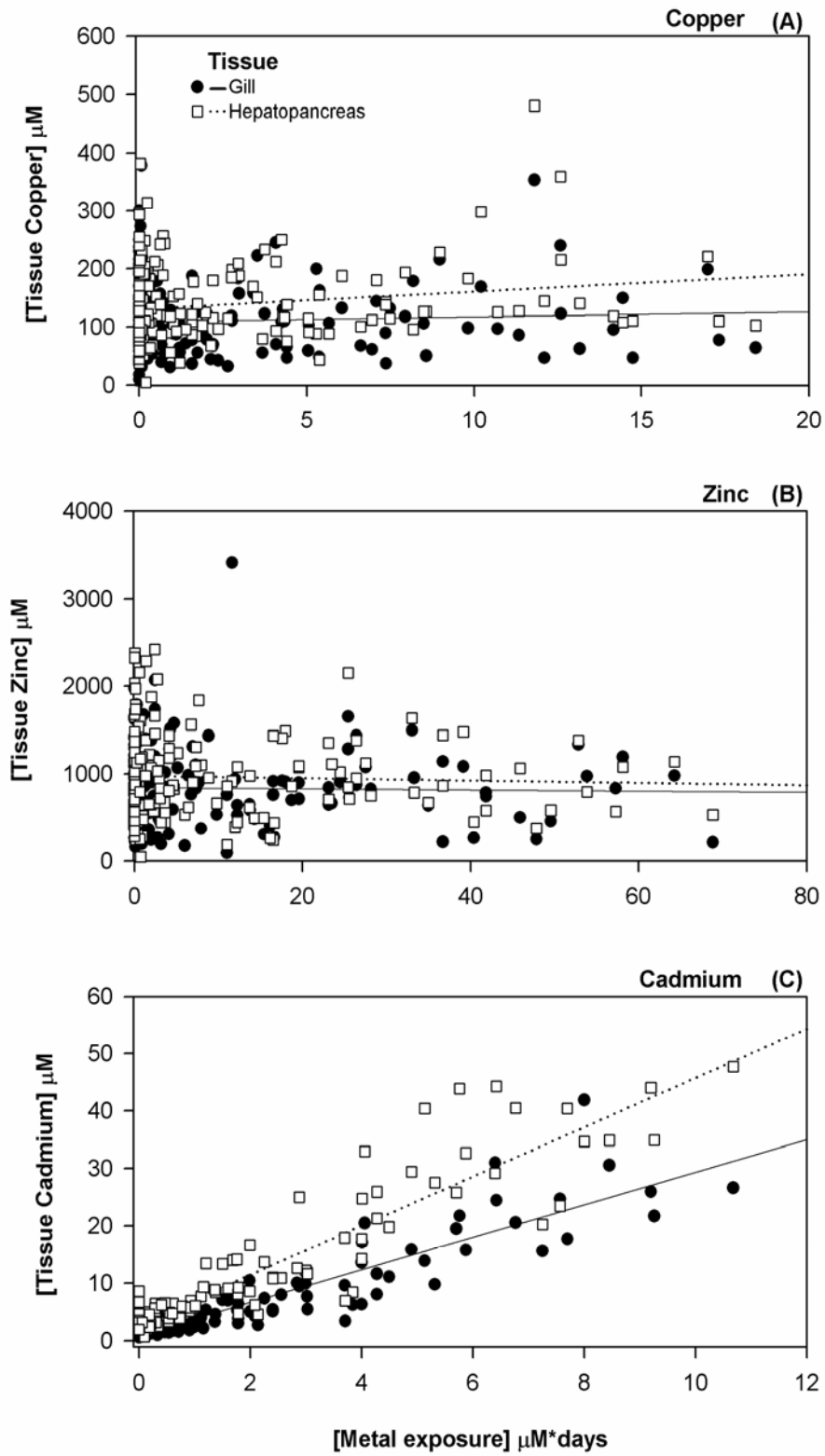
616 **Figure 5.** Sensitivities of TBARS in the gill to the input variables (metal contents, hemolymph  
617 pH, PO<sub>2</sub> and total CO<sub>2</sub>) for the best performing model 8 from the ANN analysis.

618 **Figure 6.** Theoretical projections of the response of TBARS to changes in the exposure levels of  
619 the indicated variable on the x and y axes. All variables have been scaled to their non-parametric  
620 values where 0 indicates the minimum and 1 indicates the maximum values observed in the data.  
621 (see text).

622

623

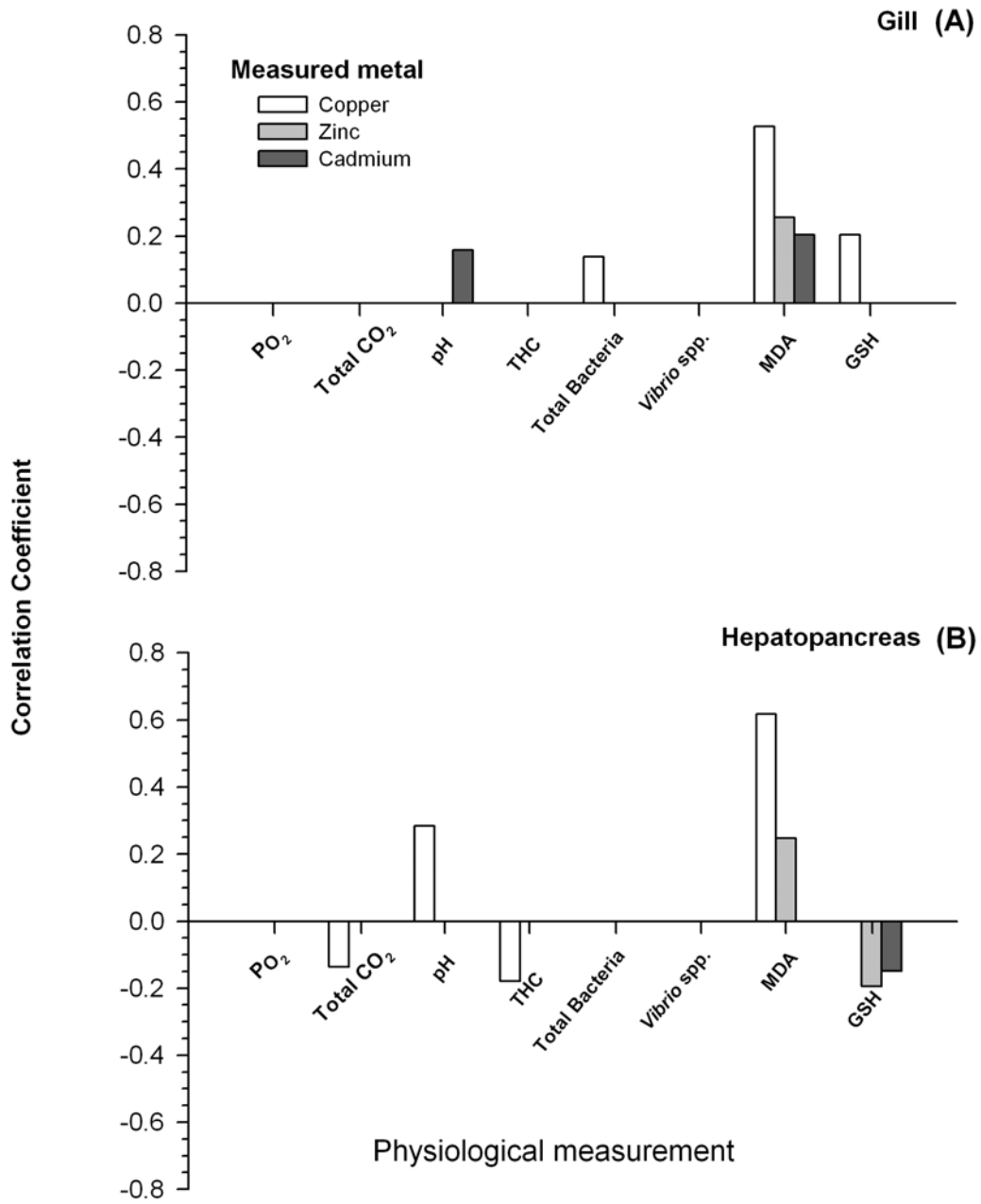
624 **Figure 1**  
625  
626





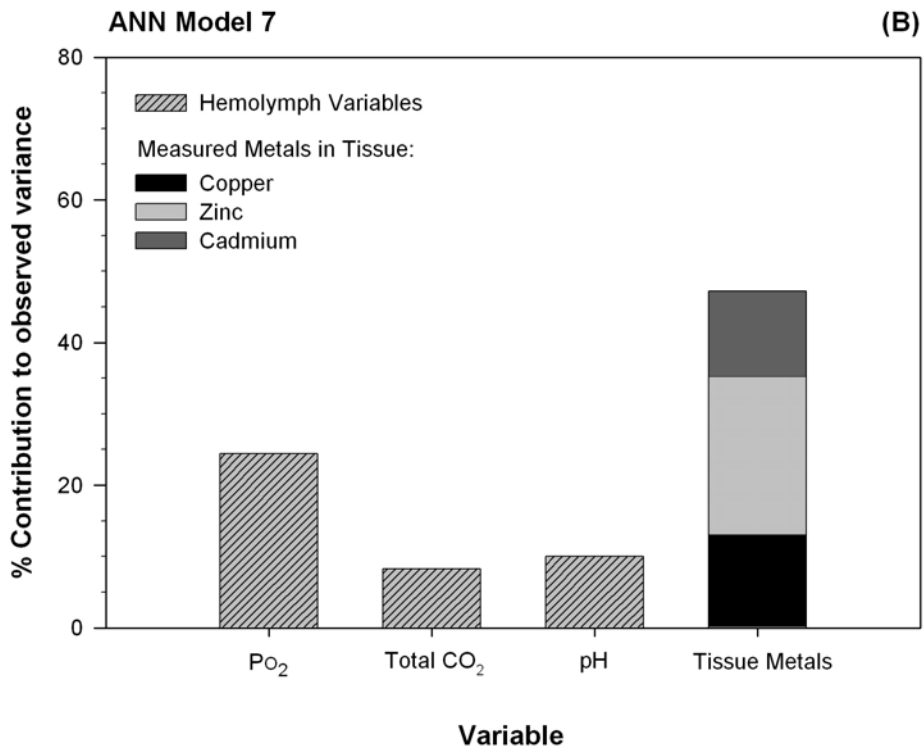
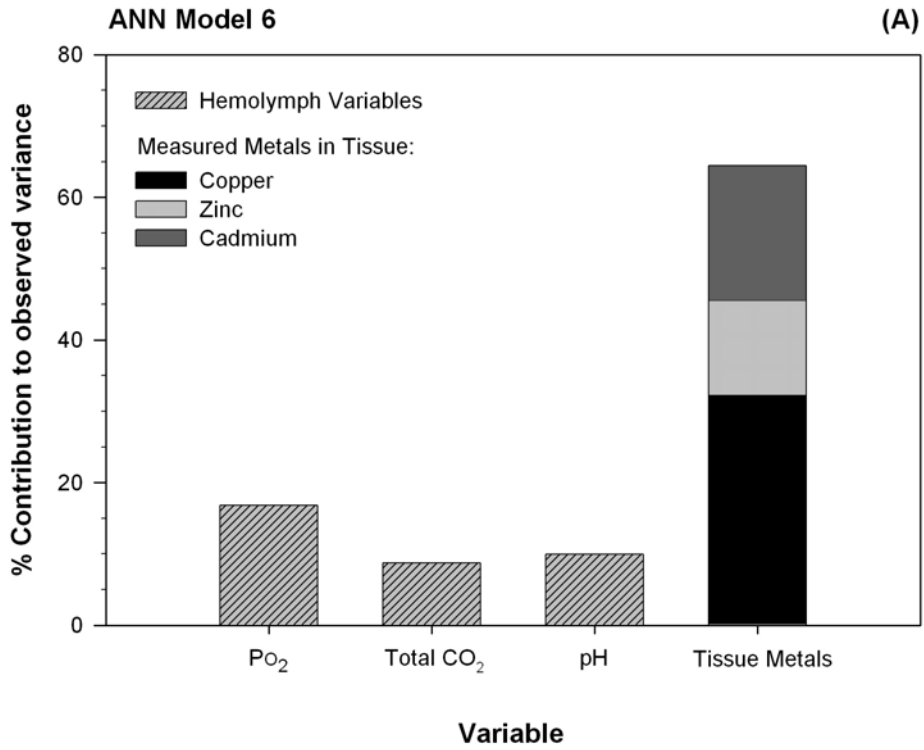


630 **Figure 3**  
631



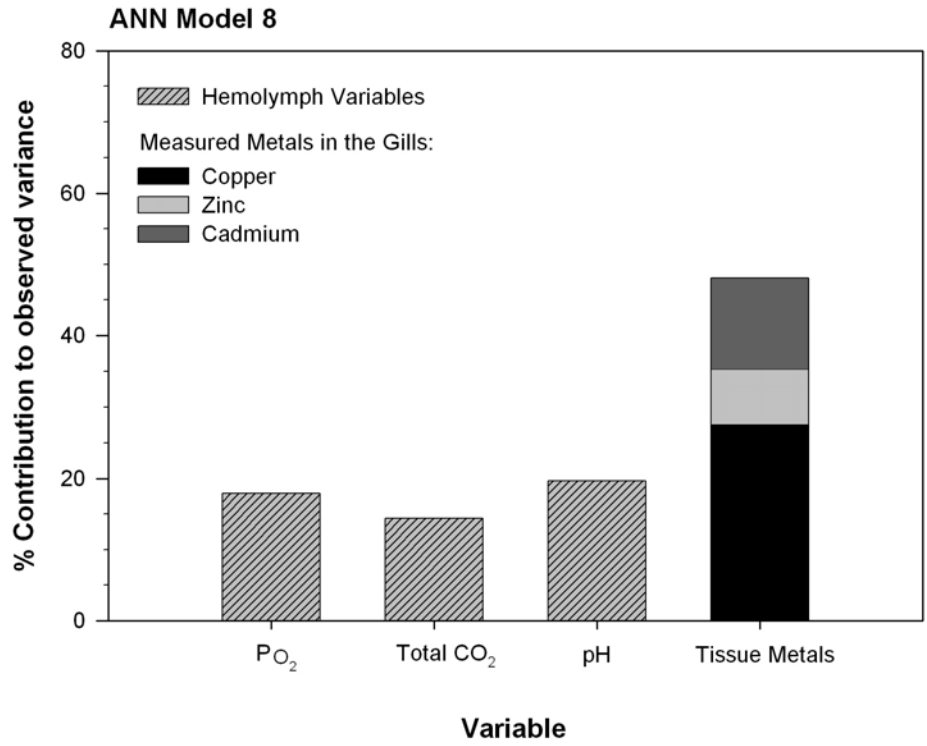
632

633 **Figure 4**  
634



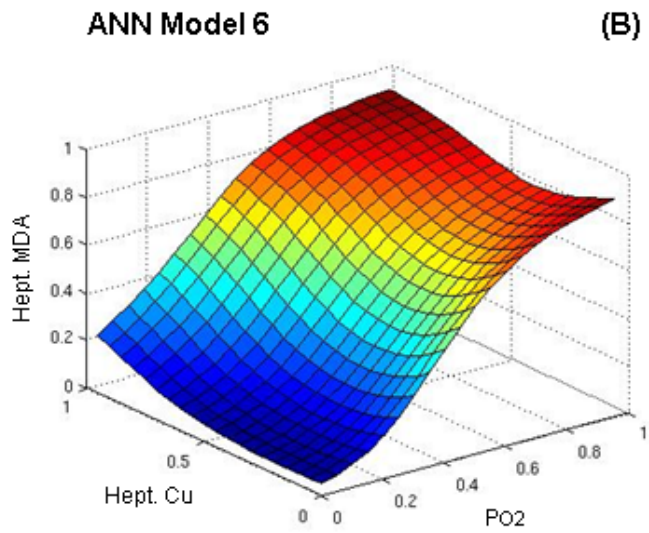
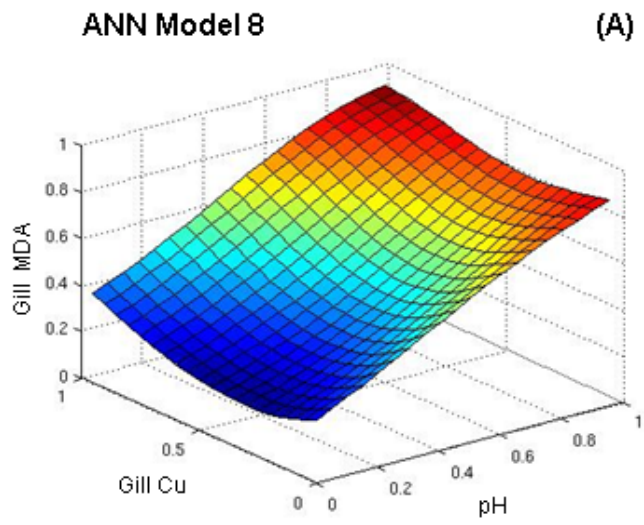
635

636 **Figure 5**



637  
638

639 **Figure 6**  
640  
641  
642



References:

- 643  
644  
645 Almeida, J.S., 2002. Predictive non-linear modeling of complex data by artificial neural  
646 networks. *Curr. Opin. Biotechnol.* 13, 72-76.
- 647 Bishop, C. M. (1996a). Neural networks: A pattern recognition perspective. In E. Fiesler and  
648 R. Beale (Eds.), *Handbook of Neural Computation*. Oxford University Press and IOP Publishing.
- 649 Bishop, C. M. (1996b). Theoretical foundations of neural networks. In P. Borchers, M. Bubak,  
650 and A. Maksymowicz (Eds.), *Proceedings of Physics Computing 96, Krakow*, pp. 500–507.  
651 Academic Computer Centre.
- 652 Bishop, C. M. (2006) *Pattern Recognition and Machine Learning*. Springer. New York, 738 pp.
- 653 Booth, C.E., McDonald, D.G., Walsh, P.J., 1984. Acid-base balance in the sea mussel, *Mytilus*  
654 *edulis*. I. Effects of hypoxia and air-exposure on hemolymph acid-base status. *Mar. Biol. Lett.* 5,  
655 347-358.
- 656 Burnett, L.E., 1988. Physiological responses to air exposure: Acid-base balance and the role of  
657 branchial water stores. *Am. Zool.* 28, 125-135.
- 658 Cannon, A.J., McKendry, I.G., 2002. A graphical sensitivity analysis for statistical climate  
659 models: application to Indian monsoon rainfall prediction by artificial neural networks and  
660 multiple linear regression models. *Int. J. Climatol.* 22, 1687-1708.
- 661 Carpenter, D.O., Arcaro, K., Spink, D.C., 2002. Understanding the human health effects of  
662 chemical mixtures. *Environ. Health Perspect.* 110, 25-42.
- 663 Chapman, R.W., Mancina, A., Beal, M. Veloso A., Rathburn, C., Blair, A., Sanger, D., Holland,  
664 A.F., Warr, G.W., and DiDonato, G. (2009) A transcriptomic analysis of land use impacts on the  
665 oyster, *Crassostrea virginica*, in the South Atlantic Bight. *Molecular Ecology* 18:2415-2425
- 666 Dailianis, S., Piperakis, S.M., Kaloyianni, M., 2005. Cadmium effects on ROS production and  
667 DNA damage via adrenergic receptors stimulation: role of Na<sup>+</sup>/H<sup>+</sup> exchanger and PKC. *Free*  
668 *Radical Research* 39, 1059-1070.
- 669 Dankbar, D.M., Dawson, E.D., Mehlmann, M., Moore, C.L., Smagala, J.A., Shaw, M.W., Cox,  
670 N.J., Kuchta, R.D., Rowlen, K.L., 2007. Diagnostic microarray for influenza B viruses. *Anal.*  
671 *Chem.* 79, 2084-2090.
- 672 Dorta, D.J., Leite, S., DeMarco, K.C., Prado, I.M.R., Rodrigues, T., Mingatto, F.E., Uyemura,  
673 S.A., Santos, A.C., Curti, C., 2003. A proposed sequence of events for cadmium-induced  
674 mitochondrial impairment. *Journal of Inorganic Biochemistry* 97, 251-257.

675 Dovzhenko, N.V., Kurilenko, A.V., Bel'cheva, N.N., Chelomin, V.P., 2005. Cadmium-induced  
676 oxidative stress in the bivalve mollusk *Modiolus modiolus*. Russ. J. Mar. Biol. 31, 309-313.

677 Elfving, T., Tedengren, M., 2002. Effects of copper on the metabolism of three species of  
678 tropical oysters, *Saccostrea cucullata*, *Crassostrea lugubris* and *C. belcheri*. Aquaculture 204,  
679 1157-1166.

680 Engel, D.W., 1999. Accumulation and cytosolic partitioning of metals in the American oyster  
681 *Crassostrea virginica*. Mar. Environ. Res. 47, 89-102.

682 Flipič, M., Fatur, T., Vudrag, M., 2006. Molecular mechanisms of cadmium induced  
683 mutagenicity. Hum. Exp. Toxicol. 25, 67-77.

684 Geret, F., Jouan, A., Turpin, V., Bebianno, M.J., Cosson, R.P., 2002a. Influence of metal  
685 exposure on metallothionein synthesis and lipid peroxidation in two bivalve mollusks: the oyster  
686 (*Crassostrea gigas*) and the mussel (*Mytilus edulis*). Aquat. Living Resour. 15, 61-66.

687 Geret, F., Serafim, A., Barreira, L., Bebianno, M.J., 2002b. Effect of cadmium on antioxidant  
688 enzyme activities and lipid peroxidation in the gills of the clam *Ruditapes decussatus*.  
689 Biomarkers 7, 242 - 256.

690 Jenny, M.J., Ringwood, A.H., Lacy, E.R., Lewitus, A.J., Kempton, J.W., Gross, P.S., Warr,  
691 G.W., Chapman, R.W., 2002. Potential Indicators of stress response identified by expressed  
692 sequence tag analysis of hemocytes and embryos from the American oyster, *Crassostrea*  
693 *virginica*. Mar. Biotechnol. 4, 81-93.

694 Khan, J., Ringér, M., Saal, L.H., Ladanyi, M., Wesermann, F., Berthold, F., Schwab, M.,  
695 Antonescu, C.R., Peterson, C., Meltzer, P.S., 2001. Classification and diagnostic prediction of  
696 cancers using gene expression profiling and artificial neural networks. Nat. Med. 7, 673-679.

697 Linder, R., Dew, D., Sudhoff, H., Theegarten, D., Remberger, K., Poppl, S.J., Wagner, M., 2004.  
698 The 'subsequent artificial neural network' (SANN) approach might bring more classificatory  
699 power to ANN-based DNA microarray analyses. Bioinformatics 20:3544-3552.

700 Macey, B.M., Achilihu, I.O., Burnett, K., Burnett, L., 2008. Effects of hypercapnic hypoxia on  
701 inactivation and elimination of *Vibrio campbellii* in the Eastern oyster, *Crassostrea virginica*.  
702 Appl. Environ. Microbiol. 74, 6077-6084.

703 Marigómez, I., Soto, M., Cajaraville, M., Angulo, E., Giamberini, L., 2002. Cellular and  
704 subcellular distribution of metals in molluscs. Microsc. Res. Tech. 56, 358-392.

705 Massabuau, J.-C., Tran, D., 2003. Ventilation, a recently described step limiting heavy metal  
706 contamination in aquatic animals. *Journal de Physique*. IV 107, 839-843.

707 Quig, D., 1998. Cysteine metabolism and metal toxicity. *Altern. Med. Rev.* 3, 262-270.

708 Ringwood, A.H., Connors, D.E., Dinovo, A., 1998. The effects of copper exposures on cellular  
709 responses in oysters. *Mar. Environ. Res.* 46, 591-595.

710 Ringwood, A.H., Connors, D.E., Keppler, C.J., Dinovo, A.A., 1999a. Biomarker studies with  
711 juvenile oysters (*Crassostrea virginica*) deployed in-situ. *Biomarkers* 4, 400-414.

712 Ringwood, A.H., Connors, D.E., Keppler, C.J., Dinovo, A.A., 1999b. Biomarker studies with  
713 juvenile oysters (*Crassostrea virginica*) deployed *in-situ*. *Biomarkers* 4, 400 - 414.

714 Roesijadi, G., 1996. Metallothionein and its role in toxic metal regulation. *Comp. Biochem.*  
715 *Physiol. C* 113, 117-123.

716 Roméo, M., Gnassia-Barelli, M., 1997. Effect of heavy metals on lipid peroxidation in the  
717 Mediterranean clam *Ruditapes decussatus*. *Comp. Biochem. Physiol. C* 118, 33-37.

718 Sanger, D.M., Holland, A.F., Scott, G.I., 1999. Tidal creek and salt marsh sediments in South  
719 Carolina coastal estuaries: I. Distribution of trace metals. *Arch. Environ. Contam. Toxicol.* 37,  
720 445-457.

721 Sexton, K., Hattis, D., 2007. Assessing cumulative health risks from exposure to environmental  
722 mixtures - three fundamental questions. *Environ. Health Perspect.* 115, 825-832.

723 Sokolova, I.M., Ringwood, A.H., Johnson, C., 2005. Tissue-specific accumulation of cadmium  
724 in subcellular compartments of eastern oysters *Crassostrea virginica* Gmelin (Bivalvia:  
725 Ostreidae). *Aquat. Toxicol.* 74, 218-228.

726 Stohs, S.J., Bagchi, D., 1995a. Oxidative mechanisms in the toxicity of metal ions. *Free Radic.*  
727 *Biol. Med.* 18, 321-336.

728 Stohs, S.J., Bagchi, D., 1995b. Oxidative mechanisms in the toxicity of metal ions. *Free Radical*  
729 *Biology and Medicine* 18, 321-336.

730 Stohs, S.J., Bagchi, D., Hassoun, E., Bagchi, M., 2000. Oxidative mechanisms in the toxicity of  
731 chromium and cadmium ions. *J. Environ. Pathol. Toxicol. Oncol.* 19, 201-213.

732 Valko, M., Morris, H., Cronin, M.T.D., 2005. Metals, Toxicity and Oxidative Stress. *Current*  
733 *Medicinal Chemistry* 12, 1161-1208.

734 Viarengo, A., 1989a. Heavy metals in marine invertebrates: mechanisms of regulation and  
735 toxicity at the cellular level. *Rev. Aquat. Sci.* 1, 295-317.

736 Viarengo, A., 1989b. Heavy metals in marine invertebrates: Mechanisms of regulation and  
737 toxicity at the cellular level. Review in Aquatic Sciences 1, 295-317.

738 Viarengo, A., Canesi, L., Pertica, M., Poli, G., Moore, M.N., Orunesu, M., 1990. Heavy metal  
739 effects on lipid peroxidation in the tissues of *Mytilus galloprovincialis* LAM. Comp. Biochem.  
740 Physiol. C 97, 37-42.

741 Wang, G., Fowler, B.A., 2008. Roles of biomarkers in evaluating interactions among mixtures of  
742 lead, cadmium and arsenic. Toxicol. Appl. Pharmacol. 233, 92-99.

743 Wang, Y., Fang, J., Leonard, S.S., Krishna Rao, K.M., 2004. Cadmium inhibits the electron  
744 transfer chain and induces Reactive Oxygen Species. Free Radical Biology and Medicine 36,  
745 1434-1443.

746 Yang, R.S.H., Dennison, J.E., 2007. Initial analyses of the relationship between "thresholds" of  
747 toxicity for individual chemicals and "interaction thresholds" for chemical mixtures. Toxicol.  
748 Appl. Pharmacol. 223, 133-138.

749

750